

Snapping Shrimp Noise Reduction using Convex Optimization for Underwater Acoustic Communication in Warm Shallow Water

Dayan Adionel Guimarães
National Institute of
Telecommunications - Inatel
Santa Rita do Sapucaí, MG, Brazil
Email: dayan@inatel.br

Lucas Silvestre Chaves
National Institute of
Telecommunications - Inatel
Santa Rita do Sapucaí, MG, Brazil
Email: lucas-srs@hotmail.com

Rausley Adriano Amaral de Souza
National Institute of
Telecommunications - Inatel
Santa Rita do Sapucaí, MG, Brazil
Email: rausley@inatel.br

Abstract—We propose an ambient noise reduction technique for underwater acoustic communication systems in warm shallow water, where the snapping shrimp impulsive noise is a common impairment. This noise is emitted at the cavitation bubble collapse caused by the claw shut, and can produce very high acoustic pressures which are responsible for the impulsiveness of the noise. The denoised signal is the solution of an unconstrained scalarized bi-criterion convex optimization problem. One of the criterions is based on the robust least-squares signal reconstruction approach, for which the sum of the Huber penalty function of the residuals is minimized. The other criterion uses a quadratic smoothing regularization term, acting on the first-difference of the denoised signal samples. It is shown that the proposed technique can significantly reduce the ambient noise and, thus, reduce the bit error rate of an underwater digital communication system.

I. INTRODUCTION

The high attenuation of electromagnetic waves, especially by sea water, is one of the most limiting factors for using radio waves for underwater communications. On the other hand, these attenuations are significantly smaller for acoustic waves, which motivates the use of acoustic signals in underwater communication systems [1, pp. 15-47], [2], [3].

Underwater acoustic communication (UWAC) systems have been used in many applications, from sound navigation and echo detection (sonar), to diver-to-diver and ship-to-diver communications, for communications with submersibles and other underwater vehicles for sea exploration, in telemetry and in underwater control systems. Applications related to underwater sensor networks are one of the most recent ones [4]–[7]. The main characteristic of UWAC systems is the use of acoustic carrier waves typically above 5 kHz. The upper limit depends on the range. As an example, for a 10 km range this upper limit is about 10 kHz. For a 100 m range, signals up to 100 kHz can be used. Some modern high speed UWAC systems for short-range communication use acoustic carriers with even higher frequencies. Transmission powers typically are on the order of 30 W or less. Transmission rates are up to a few kilobits per second in a 10 km range.

The impairments found in underwater acoustic channels are even more severe than those encountered in wireless radio

channels, representing a challenging limitation for UWAC system design. The main limiting factors are the propagation delay, multipath, attenuation and ambient noise, all with strong randomness.

The channel is subjected to a three-dimensional variability of the refractive index, leading to ray bending (refraction). This is one of the main causes of multipath and shadowing. Multipath propagation is also caused by reflections on sea surface and sea floor. Small coherence times combined with large propagation delays also impose severe limitation to the system design. For example, in a 1 km range the signal can take up to 0.66 seconds to hit the receiver. On the other hand, channel characteristics can change drastically within 0.5 seconds or less. Delay spreads can reach up to 60 ms, producing severe frequency-selective fading. Doppler shift and Doppler spread also appear, and are caused due to surface and internal wave motion and due to relative motion between receiver and transmitter. Additionally, the sound speed varies in water, mainly with depth, and depends on the water characteristics and weather conditions.

The main mechanisms of signal loss in UWAC channels are the spreading of the signal energy with distance, similar to what occurs in radio communications, absorption and scattering. Absorption is the conversion of acoustic energy into heat and it is a frequency-dependent and chemical-dependent phenomenon. Scattering occurs at sea surface and sea floor, but also on water bubbles and on small water volumes with different temperatures. Moreover, since the signal-to-noise ratio is strongly dependent on range and frequency, higher ranges mean lower available bandwidths for data transmission.

Besides the thermal noise generated at the receiver, typical ambient noise impairments in UWAC systems are generated by breaking waves, rain, marine life and ships. Among these ambient noise, in warm shallow water it is common the existence of an impulsive noise generated by snapping shrimps [8]–[11]. In this paper we propose a technique for combating the compound noise resultant from the addition of the thermal and the ambient snapping shrimp noise. Throughout the paper we interchangeably refer to this technique as noise reduction

or simply denoising. The denoised signal is sometimes referred to as the reconstructed signal.

The remaining of the paper is organized as follows: in Section II we describe the proposed noise reduction scheme. Section III presents the digital communication system model adopted for assessing the performance of the denoising process, in terms of the bit error rate (BER) versus the ratio between the average energy per bit and the noise power spectral density (E_b/N_0). Section IV provides the numerical results and Section V concludes the paper.

II. THE PROPOSED DENOISING SCHEME

An n -dimensional transmitted signal vector \mathbf{x} , under fading, is added to a vector \mathbf{n} representing the compound (thermal plus ambient) additive noise, resulting in the received vector $\mathbf{r} = \mathbf{x} + \mathbf{n}$. From this vector, the noise reduction process tries to reconstruct the transmitted signal, resulting in the estimate $\hat{\mathbf{x}}$, which is then used to detect the transmitted data. The denoised signal $\hat{\mathbf{x}}$ is the solution of the unconstrained scalarized bi-criterion convex optimization problem

$$\text{minimize } \sum_{i=1}^n \phi_{\text{hub}}(\hat{x}_i - r_i) + \delta \phi_{\text{quad}}(\hat{\mathbf{x}}), \quad (1)$$

where $\delta > 0$ parameterizes the trade-off between fitting (governed by the first term) and smoothness (governed by the second term). The Huber penalty function with shape parameter M is [12, p. 299]

$$\phi_{\text{hub}}(u) = \begin{cases} u^2 & |u| \leq M \\ M(2|u| - M) & |u| > M \end{cases}, \quad (2)$$

and the quadratic smoothing function is [12, p. 312]

$$\phi_{\text{quad}}(\hat{\mathbf{x}}) = \sum_{i=1}^{n-1} (\hat{x}_{i+1} - \hat{x}_i)^2. \quad (3)$$

The reasoning behind the proposed denoising technique goes as follows: it is known that when the Huber penalty function is applied to a linear regression problem, the result is robust against data outliers, and that is the reason for giving the name *robust least-squares* to such approach. From the perspective of the compound noise present in UWAC communications, the impulsive noise samples can be seen as outliers within the received signal samples. The solution of the least squares in the linear regression problem can be seen as a linear approximation of a smoothed reconstructed signal segment. Then, by combining a robust least-squares fitting with a smoothing process, the reconstructed signal will not depart too much from the smoothed one by the influence of the impulsive noise. In other words, the quadratic function in (1) will produce a smooth reconstructed signal that, due to the influence of the first term, does not care too much about the presence of the impulsive noise, depending on the value of δ : a smaller δ acts in favor of a better fit between the corrupted and the reconstructed signal, in the Huber measure sense; a larger δ acts in favor of a smoother reconstructed signal. To the best of our knowledge, no such approach has been adopted

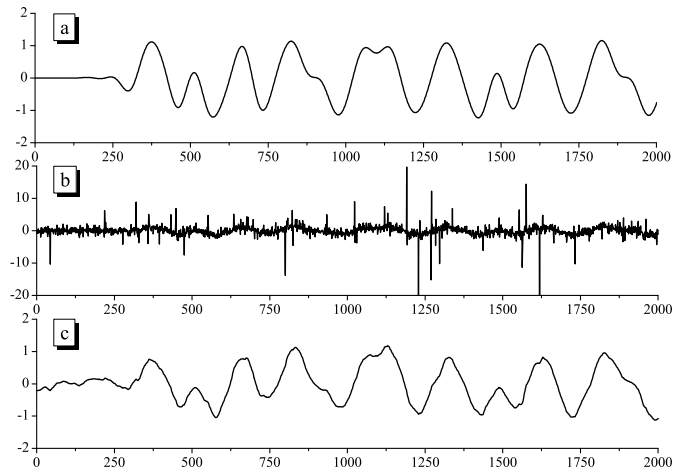


Fig. 1. Examples of: a) the transmitted signal vector \mathbf{x} , b) the corrupted received signal vector \mathbf{r} , and c) the reconstructed signal vector $\hat{\mathbf{x}}$

so far for combating the ambient noise in underwater acoustic communication systems.

For illustration purpose only, Figure 1 shows 2000-point vectors from this signal denoising process. Notice that the received vector is under a heavy noise condition, with strong impulsiveness. Nonetheless, the denoised signal is noticeably free from impulsive noise and from most of the thermal noise. Yet, the reconstructed signal is free from the typical time dispersion the would be produced if conventional filtering were used as a means for noise reduction. An efficient filtering (in terms of noise reduction) would inevitably be accompanied by intersymbol interference, which would prevent the reduction of the symbol error rate.

III. SYSTEM MODEL FOR PERFORMANCE ANALYSIS

The vector \mathbf{x} represents a transmitted signal whose rate of amplitude variations is much slower than those present in the compound noise vector, so that the denoising process works as desired. This condition can be met by modulated and filtered UWAC signals due to the fact that, besides the smoothness produced by filtering, the carrier in these systems is an acoustic wave, typically with frequency on the order of a few tens of kilohertz [1, pp. 15-47]. Moreover, the frequency content of the snapping shrimp impulsive noise easily reaches 250 kHz [9], which means that, indeed, its rate of variation is much larger than the rate of variation of typical modulated and filtered transmitted signals used in UWAC systems.

Besides the compound noise, UWAC signals are also subjected to fading, even in short-range communications where the observed fading is similar, but slightly less severe than predicted by the Rayleigh distribution [3, p. 73]. Thus, it is mandatory to consider the effect of the fading in the performance of an UWAC system.

Aiming at adhering to the above requirements, we have adopted the system model shown in Figure 2. A root-raised cosine (RRC) filtered binary phase-shift keying (BPSK) signal is transmitted over a Rayleigh fading channel with compound

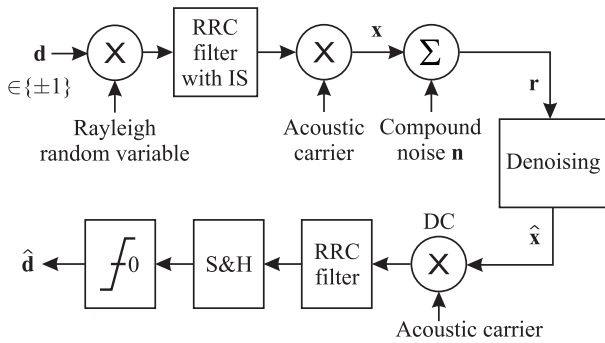


Fig. 2. System model for performance analysis

(thermal plus ambient impulsive) noise. The multiplicative fading effect is modeled as the multiplication of the binary ± 1 data by a Rayleigh random variable with unitary second moment, constant during the symbol duration and independent from symbol to symbol - notice that this is a simple way of guaranteeing that, in this waveform channel model, the fading component affecting the decision variable is Rayleigh-distributed, allowing for checking the performance against theoretical results and for speeding-up the system simulation. If a waveform fading channel were adopted instead, the fading envelope variations should be very slow to be in close agreement with the common assumption of constant fading during the symbol interval. This would render the simulation time last too long for guaranteeing that the average fading effect manifests.

The transmit RRC filter is equipped with an inverse sinc (IS) equalization, since the input pulses are rectangular. The compound noise waveform is generated as an $S\alpha S$ (symmetric α -stable) process, which adequately models the UWAC ambient noise and the presence of the snapping shrimp noise [3], [10]. The carrier signals used for modulation and down-conversion (DC) to base-band are cosine waves with frequency in the acoustic range. The output of the RRC receive filter (with no IS equalization) is sampled and held (S&H) and the results are compared with zero so that the transmitted symbols are estimated. Finally, transmitted and estimated symbols are compared for bit (symbol) error rate computation.

IV. NUMERICAL RESULTS

In this section we give numerical results aiming at assessing the performance of the proposed convex optimization denoising scheme. The benchmarks are the performance of the optimum receiver for the AWGN (additive white Gaussian noise) channel and the performance of a suboptimal receiver equipped with a non-linear (clipping) device operating in the impulsive noise environment. Channel fading is present in all cases under analysis.

The system model in Figure 2 was implemented in Matlab[®] and validated by comparing its performance with the theoretical performance of a BPSK modem over the Rayleigh-AWGN channel for several values of E_b/N_0 . A perfect agreement has been observed. In this case the $S\alpha S$ process has been modified

to a Gaussian process by setting the characteristic exponent $\alpha = 2$ [3, p. 22].

To speedup computations, we have chosen a simulation sampling frequency of 10 kilosamples per second, meaning that the impulsive and thermal noise bandwidths are equal to 5 kHz. Since the bandwidth of the actual snapping shrimp impulsive noise can reach even beyond 250 kHz [9], 500 kilosamples per second would suffice for most of the practical applications. Then, a factor of 50 is observed between this sampling frequency and the simulation sampling frequency. To maintain this proportion in simulations, we have used a carrier wave with frequency of 200 Hz, which corresponds to an acoustic carrier wave of 10 kHz. The symbol rate has been also downsized from a typical value of 5 kbit/s to 100 bit/s, that is, the symbol duration corresponds to 2 carrier periods and 100 simulation samples. The $S\alpha S$ process was generated with α between 1.5 and 1.9, where $\alpha = 1.5$ simulates a stronger snapping shrimp noise component [3]. The scale parameter γ of the $S\alpha S$ process has been adjusted according to the desired E_b/N_0 as follows:

$$\gamma = \frac{\sigma}{\sqrt{2}} = \frac{\sqrt{N_0}}{2} = \sqrt{\frac{E_b}{4 \times 10^{\frac{E_b/N_0}{10}}}}, \quad (4)$$

where σ is the standard deviation of the Gaussian noise component in the $S\alpha S$ process, $E_b = P/R_b$ is a function of the average received signal power P and the bit rate R_b , and E_b/N_0 is in dB. It is worth noting that this computation of γ is exact only when $\alpha = 2$, the unique case in which the variance of the $S\alpha S$ process is finite. Then, one must consider that the actual value of E_b/N_0 is approximately equal to the desired value when $\alpha \neq 2$.

The RRC filters have a roll-off 0.2 and $100k$ taps, where k is the number of symbol intervals spanned by their impulse responses. We have adopted $k = 10$ so that most of the impulse response tail is taken into account. The simulation operates in a frame-by-frame basis and the frame duration defines the dimension of the vectors described in Section II and in practice would be defined by the tradeoff between this dimension and the amount of time needed to solve the optimization problem (1) before a new frame is loaded. If the received data does not need to be available in real time, the restrictions on the frame duration and on the time to solve (1) are relaxed, which is the case of some underwater sensor network applications [7]. Here we have used a frame size $n = 1500$ samples, aiming at maximizing the ratio between the number of transmitted bits per frame and the simulation end time: small values of n reduce the time to solve the optimization problem, but diminishes number of bits in a frame, causing the increase of the number of transmitted frames, thus increasing the simulation end time; higher values of n increase the number of transmitted bits per frame, but increase in a higher proportion the time to solve the optimization problem, which renders the simulation end time to increase.

Problem (1) has no analytical solution and was solved using CVX, a Matlab-based system for modeling and solving convex

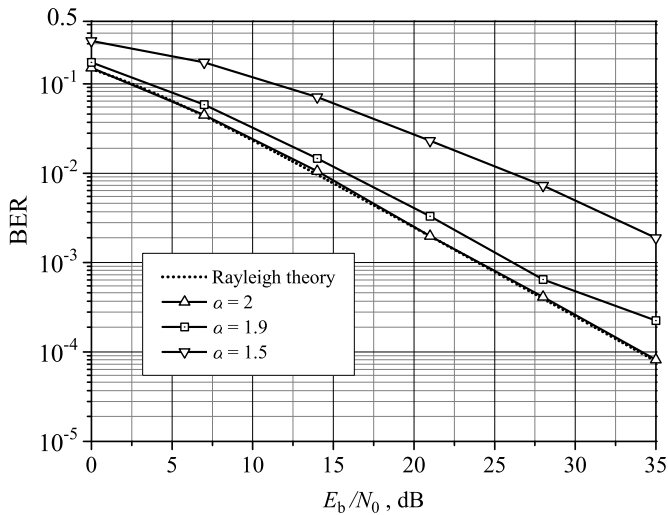


Fig. 3. System performance without denoising for variable α

optimization problems [13]. The values of δ in (1) were chosen so as to move the BER versus E_b/N_0 curve as much as possible to the left. They were chosen to be adapted with the value of E_b/N_0 or fixed, as we shall see from the simulation results. The shaping parameter of the Huber penalty function (2) was set to $M = 0.009$.

A. No Noise Reduction

Figure 3 shows the performances of the UWAC system in the presence of the S α S noise, under different values of the characteristic exponent α . For $\alpha = 2$ we have a Gaussian-only noise and the performance closely approximates the theoretical result; $\alpha = 1.5$ and $\alpha = 1.9$ represents the strongest and weakest snapping shrimp noise situation, respectively. Notice that the performance can be severely degraded if no countermeasure is applied against the impulsive nature of the snapping shrimp noise.

B. Noise Reduction via Clipping

There are several methods for designing locally optimal and suboptimal detectors for signals in the presence of the S α S noise. One of these methods is implemented by introducing a nonlinear device before a matched filter or correlator detector [3, Chap. 4]. However, this method requires *a priori* knowledge of the impulsive characteristics of the noise and are generally not suitable for signals where such characteristics are time-varying. Here we adopt a device with the following suboptimal transfer function:

$$y = \begin{cases} x & \text{if } |x| \leq c \\ \text{sign}(x)c & \text{if } |x| > c \end{cases}, \quad (5)$$

where x is the input of the clipping device, y is the output, and c is the clipping value. This function keeps low amplitude signals with no distortion, while clipping large impulsive noise and, thus, improving detector performance. However, when the signal is also strong, it gets clipped as well and the performance of the detector drops. To avoid this, the clipping value

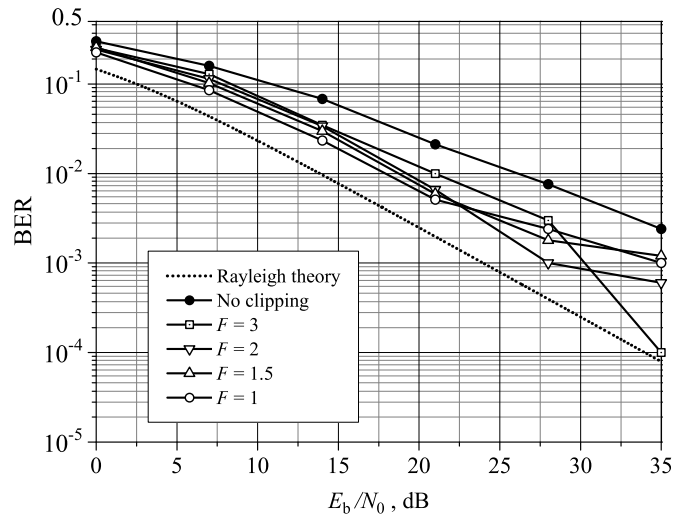


Fig. 4. Performance of the adaptive clipping with the empirical nonlinear-device denoising (END) for $\alpha = 1.5$

c should be adapted according to the standard deviation σ of the Gaussian component of the S α S process and on the actual amplitude of the received signal, which depends on the fading factor β that accounts for the RRC-filtered Rayleigh random variable and on the amplitude of the modulated and filtered signal, which in turn depends on the roll-off of the RRC filter and on the data sequence. Disregarding the data sequence, the clipping value should be $c = k_1\sigma + k_2\beta\sqrt{2P}$, where k_1 and k_2 are chosen so as to guarantee that the desired signal is not clipped and that the Gaussian noise around this signal is not severely clipped. However, in the high signal-to-noise ratio regime the data-dependent signal amplitude variations should be tracked more precisely to produce noticeable improvement. Then, in this regime the above suboptimal value of c will not be capable of correctly representing the ideal clipping value, reducing the performance of the technique.

Clearly, the above suboptimal adaptation can not be easily implemented in practice, since several parameters should be estimated or known *a priori*. Then, we have considered an alternative adaptation of c according to the time-series average power ρ of the samples received in each frame, after down-conversion, according to the simple empirical rule $c = F\sqrt{\rho}$, being F a calibration factor. We call it the empirical nonlinear-device denoising (END) technique. Figure 4 gives numerical results showing the performances of this clipping rule for some values of F and $\alpha = 1.5$. One can see that if F is adjusted to produce a good performance in the low E_b/N_0 region, the performance at higher values of E_b/N_0 is penalized. If F is adjusted to produce a satisfactory performance in the high E_b/N_0 regime, the performance at lower values of E_b/N_0 is penalized.

C. Noise Reduction via Convex Optimization

In this subsection we address the performance of the proposed denoising technique, which we name convex optimization denoising (COD) for notational simplicity. Figure

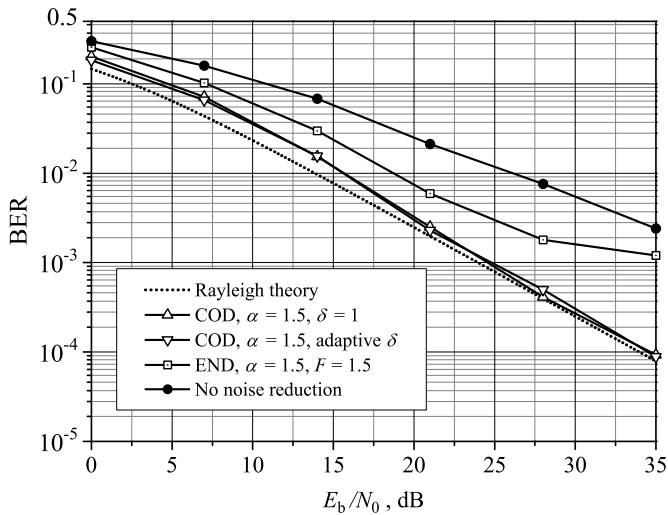


Fig. 5. Performance of the proposed (COD) and empirical (END) techniques for $\alpha = 1.5$, adaptive $\delta = 0.6, 0.6, 0.8, 1.2, 1.4, 1.5$ and fixed $\delta = 1$

5 shows the results considering a strong impulsive noise ($\alpha = 1.5$) situation. The performance of the COD consider that the regularization factor is fixed at $\delta = 1$ and adapted as $\delta = 0.6, 0.6, 0.8, 1.2, 1.4, 1.5$, respectively for the values of $E_b/N_0 = 0, 7, 14, 21, 28, 35$ dB (this adaptation was made based on the minimum mean square error between the transmitted and the reconstructed signal). The performance of the receiver equipped with the END for $F = 1.5$, i.e. considering the intermediate curve given in Figure 4 is also reproduced here. We notice that the COD outperforms the END for all values of E_b/N_0 . A gain larger than 10 dB can be achieved for a BER of 10^{-3} with respect to the performance with the END. Moreover, we observe that the performance of the COD does not vary too much from the situation of fixed to adaptive regularization factor, which means that the proposed denoising scheme is robust against variations in the signal-to-noise ratio. Then, the value of δ can be the same for any value of E_b/N_0 , simplifying receiver calibration.

V. CONCLUSIONS

We have proposed an ambient noise reduction technique for underwater acoustic communication systems in warm shallow water, where the snapping shrimp impulsive noise is common and severely degrades the system performance. We have seen that the proposed technique can significantly reduce the BER in the presence of strong impulsive noise, with little or no adaptation to the signal-to-noise ratio. We have also seen that the technique does not demand that the impulsive noise is detected to be subsequently processed, i.e. it is transparent to the presence or absence of impulsive-like noise in the received signal. Nevertheless, it has the limitation of the time required to solve the corresponding optimization problem, a drawback that might not exist in several underwater sensor networks applications. In these applications, the received data can be processed in a long-term fashion by a receiving node with

high computation capability. Moreover, real-time applications [7] can be envisaged in the near future due to the proliferation of the real-time convex optimization concept [14].

While real-time convex optimization is not widespread to the point of being applicable to the problem at hand, an attempt to speed-up the solution of the convex optimization problem would be by trying accelerated first-order methods [15]. This is because the interior-point methods adopted in CVX are computationally expensive for the the problem (1), mainly due to the Hubber function. Moreover, it would be of value to compare the performance and the complexity of the solution proposed here with other solutions to the shrimp noise reduction problem, for example [16] and [17].

REFERENCES

- [1] J. G. Proakis, Ed., *Wiley Encyclopedia of Telecommunications*. John Wiley & Sons, Inc., 2003, vol. 1.
- [2] A. Quazi and W. Konrad, "Underwater acoustic communications," *Communications Magazine, IEEE*, vol. 20, no. 2, pp. 24–30, March 1982.
- [3] M. Chitre, "Underwater acoustic communications in warm shallow water channels," Ph.D. dissertation, National University of Singapore, 2006.
- [4] J. Heidemann, W. Ye, J. Wills, A. Syed, and Y. Li, "Research challenges and applications for underwater sensor networking," in *Wireless Communications and Networking Conference, 2006. WCNC 2006. IEEE*, vol. 1, April 2006, pp. 228–235.
- [5] F. Yunus, S. H. S. Ariffin, and Y. Zahedi, "A survey of existing medium access control (mac) for underwater wireless sensor network (uwsn)," in *Mathematical/Analytical Modelling and Computer Simulation (AMS), 2010 Fourth Asia International Conference on*, May 2010, pp. 544–549.
- [6] M. Erol-Kantarci, H. Moutah, and S. Oktug, "A survey of architectures and localization techniques for underwater acoustic sensor networks," *IEEE Commun. Surveys Tuts.*, vol. 13, no. 3, pp. 487–502, Third 2011.
- [7] I. A. Dario, I. F. Akyildiz, D. Pompili, and T. Melodia, "Underwater acoustic sensor networks: Research challenges," *Ad Hoc Networks (Elsevier)*, vol. 3, pp. 257–279, 2005.
- [8] B.-N. Kim, J. Hahn, B. K. Choi, and B.-C. Kim, "Acoustic characteristics of pure snapping shrimp noise measured under laboratory conditions," *Proceedings of Symposium on Ultrasonic Electronics*, vol. 30, pp. 167–168, 2009.
- [9] M. Legg, A. Zaknich, A. Duncan, and M. Greening, "Analysis of impulsive biological noise due to snapping shrimp as a point process in time," in *OCEANS 2007 - Europe*, June 2007, pp. 1–6.
- [10] M. Chitre, J. Potter, and S.-H. Ong, "Optimal and near-optimal signal detection in snapping shrimp dominated ambient noise," *IEEE J. Ocean. Eng.*, vol. 31, no. 2, pp. 497–503, Apr. 2006.
- [11] J. S. G. Panaro, F. R. B. Lopes, L. M. Barreira, and F. E. Souza, "Underwater acoustic noise model for shallow water communications," in *Proceedings of the XXX Brazilian Telecommunications Symposium, SBrT12*, September 2012.
- [12] S. Boyd and L. Vandenberghe, *Convex Optimization*. Cambridge University Press, 2004.
- [13] M. Grant and S. Boyd, "CVX: Matlab software for disciplined convex programming, version 2.1," <http://cvxr.com/cvx>, Mar. 2014.
- [14] J. Mattingley and S. Boyd, "Real-time convex optimization in signal processing," *Signal Processing Magazine, IEEE*, vol. 27, no. 3, pp. 50–61, May 2010.
- [15] T. Jensen, *First-order Convex Optimization Methods for Signal and Image Processing*. Multimedia Information and Signal Processing, Department of Electronic Systems, Aalborg University, 2011. [Online]. Available: <http://books.google.com.br/books?id=15xHnwEACAAJ>
- [16] H. Ou, J. S. Allen, and V. L. Syrmos, "Frame-based time-scale filters for underwater acoustic noise reduction," *Oceanic Engineering, IEEE Journal of*, vol. 36, no. 2, pp. 285–297, 2011.
- [17] T. Suzuki, H. M. Tran, and T. Wada, "An underwater acoustic OFDM communication system with shrimp (impulsive) noise cancelling," in *Computing, Management and Telecommunications (ComManTel), 2014 International Conference on*. IEEE, 2014, pp. 152–156.